THE JOURNAL OF BIOLOGICAL CHEMISTRY VOL. 288, NO. 24, pp. 17495–17507, June 14, 2013

Activation of Asparaginyl Endopeptidase Leads to Tau Hyperphosphorylation in Alzheimer Disease*

Received for publication, December 17, 2012, and in revised form, April 23, 2013 Published, JBC Papers in Press, May 2, 2013, DOI 10.1074/jbc.M112.446070

Gustavo Basurto-Islas, Inge Grundke-Iqbal†, Yunn Chyn Tung, Fei Liu, and Khalid Iqbal[1]

From the Department of Neurochemistry, New York State Institute for Basic Research in Developmental Disabilities, Staten Island, New York 10314-6399

Background: Abnormal hyperphosphorylation of the microtubule-associated protein Tau is a hallmark of Alzheimer disease.
Results: Acidosis of the brain activates and translocates asparaginyl endopeptidase from neuronal lysosomes to the cytoplasm where it leads to Tau hyperphosphorylation by inhibition of protein phosphatase 2A through cleavage of its inhibitor 2 into two active fragments.
Conclusion: Activated asparaginyl endopeptidase causes Tau pathology.
Significance: Brain acidosis can trigger Tau hyperphosphorylation.

Neurofibrillary pathology of abnormally hyperphosphorylated Tau is a key lesion of Alzheimer disease and other tauopathies, and its density in the brain directly correlates with dementia. The phosphorylation of Tau is regulated by protein phosphatase 2A, which in turn is regulated by inhibitor 2, I_2^{PP2A}. In acidic conditions such as generated by brain ischemia and hypoxia, especially in association with hyperglycemia as in diabetes, I_2^{PP2A} is cleaved by asparaginyl endopeptidase at Asn-175 into the N-terminal fragment (I_{2NTF}) and the C-terminal fragment (I_{2CTF}). Both I_{2NTF} and I_{2CTF} are known to bind to the catalytic subunit of protein phosphatase 2A and inhibit its activity. Here we show that the level of activated asparaginyl endopeptidase is significantly increased, and this enzyme and I_2^{PP2A} translocate, respectively, from neuronal lysosomes and nucleus to the cytoplasm where they interact and are associated with hyperphosphorylated Tau in Alzheimer disease brain. Asparaginyl endopeptidase from Alzheimer disease brain could cleave GST-I_2^{PP2A}, except when I_2^{PP2A} was mutated at the cleavage site Asn-175 to Gln. Finally, an induction of acidosis by treatment with kainic acid or pH 6.0 medium activated asparaginyl endopeptidase and consequently produced the cleavage of I_2^{PP2A}, inhibition of protein phosphatase 2A, and hyperphosphorylation of Tau, and the knockdown of asparaginyl endopeptidase with siRNA abolished this pathway in SH-SY5Y cells. These findings suggest the involvement of brain acidosis in the etiopathogenesis of Alzheimer disease, and asparaginyl endopeptidase-I_2^{PP2A}-protein phosphatase 2A-Tau hyperphosphorylation pathway as a therapeutic target.

Alzheimer disease (AD)[2] is characterized by neuronal degeneration associated with the abnormal hyperphosphorylation and aggregation of the microtubule associated protein Tau and extracellular deposits of Aβ. Aggregation of both the altered Tau and amyloid β have been shown to be associated with brain acidosis (1–4). Furthermore, ischemia and hypoxia, especially in association with hyperglycemia, lower brain pH. The fall in pH may result in a decrease in cellular metabolic activity, accumulation of acidic metabolites in the cell, and modulation of lysosomal enzymes (5–7).

Lysosomal enzyme, asparaginyl endopeptidase (AEP, also known as legumain), is a cysteine proteinase that is synthesized as a zymogen (pro-AEP, 56 kDa) and autocatalytically processed into active AEP under acidic conditions. Processing of AEP requires sequential removal of the C- and N-terminal propeptides at different pH thresholds to generate 46-kDa (active pro-AEP) and 36-kDa (active AEP) active enzymes (8, 9). AEP has multiple roles depending on substrate specificity such as initiator of invariant chain processing during MHC class II-mediated antigen presentation (10), inducer of cell migration (11, 12), and modulator of processes such as proliferation (13) and both pro-death and pro-survival functions using apoptotic mechanisms (14). The variety of roles of AEP is due to its ability to proteolyse multiple substrates, including among others the extracellular matrix protein fibronectin (15), progelatinase (16), and cathepsin H, B, and L (17). One protein shown to be cleaved by AEP during acidosis in both cellular and animal models of stroke is inhibitor 2 (I_2^{PP2A}) of protein phosphatase 2A (PP2A) (18, 19).

I_2^{PP2A} has been described as a potent inhibitor of PP2A (20), a phosphatase that accounts for ~70% of the adult human brain phosphoserine/phosphothreonine Tau protein phosphatase activity (21). PP2A activity is compromised in AD and is believed to be a cause of the Tau neurofibrillary pathology (22–

* This work was supported, in whole or in part, by National Institutes of Health Grant AG019158. This work was also supported by the New York State Office of People with Developmental Disabilities.
† Inge Grundke-Iqbal, who co-supervised the study and participated in the preparation of the manuscript, died on September 22, 2012.
[1] To whom correspondence should be addressed: Dept. of Neurochemistry, Inge Grundke-Iqbal Research Floor, New York State Inst. for Basic Research in Developmental Disabilities, 1050 Forest Hill Rd., Staten Island, NY 10314. Tel.: 718-494-5259; E-mail: khalid.iqbal.ibr@gmail.com.

[2] The abbreviations used are: AD, Alzheimer disease; AEP, asparaginyl endopeptidase, also known as legumain; I_2^{PP2A}-M, mutant I_2^{PP2A}; ID, immunodepleted; IP, immunoprecipitated/immunoprecipitation; PP2A, protein phosphatase 2A; aCSF, artificial cerebrospinal fluid; siAEP, siRNA against human AEP.

24). I_2^{PP2A}, also known as SET, TAF-1β, or PHAP II, is a 39-kDa protein widely expressed in different tissues and mainly localized in the nucleus (25). Despite its nuclear location, I_2^{PP2A} is able to move freely to the cytoplasm to induce cell migration (26, 27). Moreover, I_2^{PP2A} is involved in the control of cell cycling (28), gene transcription (29), and protection of histone from acetylation (30), and it is even suggested that I_2^{PP2A} is a part of the neuronal apoptotic pathway related to AD (31). I_2^{PP2A} was found to be selectively cleaved at Asn-175 in AD brain (32), and the PP2A activity is inhibited by the interaction of the two I_2^{PP2A} cleavage products: N- and C-terminal fragments (I_{2NTF} and I_{2CTF}) with the PP2A catalytic subunit PP2Ac (33). Furthermore, expression of I_{2NTF} and I_{2CTF} in rat brain induced inhibition of PP2A activity, abnormal hyperphosphorylation and aggregation of Tau, intraneuronal accumulation of Aβ, and neurodegeneration (34, 35). If the PP2A activity is decreased in AD by its interaction with either the I_{2NTF} or I_{2CTF} fragment, then AEP can be a responsible enzyme that starts this pathological mechanism.

In this study, we show that AEP is highly activated in AD brain and is translocated from neuronal lysosomes to the cytoplasm where I_2^{PP2A} is also translocated from the nucleus, suggesting that the cleavage of I_2^{PP2A} at Asn-175 by AEP takes place mainly in this compartment. Furthermore, we show that the cleavage of I_2^{PP2A} by AEP can trigger one of the main pathways for the AD-type hyperphosphorylation of Tau.

EXPERIMENTAL PROCEDURES

Human Brain Tissue—Frozen tissue samples of frontal cortices from autopsied and histopathologically confirmed AD and control cases were obtained from the Sun Health Research Institute Brain Donation Program (Sun City, AZ) and from the Harvard Brain Bank of McLean Hospital (Belmont, MA). The tissue was homogenized to 10% (w/v) final concentration in cold buffer containing 50 mM Tris-HCl, pH 7.4, 8.5% sucrose, 2 mM EDTA, 2 mM EGTA, 10 mM β-mercaptoethanol, 5 mM benzamidine, 0.5 mM 4-(2-aminoethyl) benzenesulfonyl fluoride, 4 μg/ml pepstatin A, and 10 μg/ml each of aprotinin and leupeptin, 20 mM β-glycerolphosphate, 100 mM sodium fluoride, 1 mM sodium vanadate, and 100 nM okadaic acid and used for Western blots. The ages, genders, and postmortem delays of the AD and control cases are listed in Table 1. The use of frozen human brain tissue was in accordance with National Institutes of Health guidelines and was approved by the Institutional Review Board of the New York State Institute for Basic Research in Developmental Disabilities. Formalin-fixed AD and control brain paraffin-embedded sections (5-μm thickness) were used for immunohistochemistry.

Subcellular Fractionation—Lysosomes, nuclei, and cytosol were isolated from human brain tissue as previously described (36). Briefly 5 g of brain tissue was homogenized in 3 volumes of cold homogenizing buffer containing 0.32 M sucrose, 1 mM EDTA disodium, 10 mM HEPES, pH 7.4, using Potter-Elvehjem homogenizer with 5–10 gentle strokes at 500 rpm. Homogenates were centrifuged at 750 $\times$ *g* for 10 min in a swinging bucket rotor. The supernatant was kept, and the pellet was resuspended with 3–4 strokes in 10 ml of the buffer and centrifuged as above. The second supernatant was combined with the previous one, and the pellet was saved as the nuclear fraction. The pooled supernatant was centrifuged at 20,000 $\times$ *g* for 10 min in a fixed angle rotor. The pellet was saved, the supernatant was centrifuged at 105,000 $\times$ *g* for 1 h, and the resulting supernatant was saved as the cytosolic fraction. The 20,000 $\times$ *g* pellet from above was resuspended with 3–4 strokes in 20 ml of the homogenizing buffer and centrifuged at 20,000 $\times$ *g* for 10 min. The supernatant was discarded, and the pellet was resuspended with 3–4 strokes in 4 ml of the buffer and layered over 36 ml of 27% (v/v) Percoll and centrifuged at 20,000 $\times$ *g* for 90 min. The lysosomal band in the bottom 1–2 ml was collected and centrifuged at 100,000 $\times$ *g* for 1 h, and the turbid layer of lysosomes just above the pellet was collected. After protein quantification, the samples were resuspended in Laemmli buffer and used for Western blots.

TABLE 1
AD and control cases from which the brain tissue was used in this study
F, female; M, male; PMI, postmortem interval.

Case	Age at death	Gender	PMI
	years		*h*
Control 1	83	F	3.25
Control 2	85	F	2.75
Control 3	82	F	2
Control 4	70	F	2
Control 5	82	F	2.25
Control 6	73	M	2
Control 7	78	M	1.66
Control 8	85	M	3.16
Control 9	80	M	3.25
Control10	80	M	2.16
Control 11	65	F	<6
Control 12	82	M	6
Control 13	84	F	4.25
Control 14	78	M	3
Mean±S.D.	79.07 ± 5.92		2.90 ± 1.18
AD 1	83	F	3
AD 2	79	F	1.5
AD 3	73	F	2
AD 4	74	F	2.83
AD 5	74	M	2.75
AD 6	81	M	3
AD 7	76	M	2.33
AD 8	72	M	2.5
AD 9	80	F	2.9
AD 10	77	M	5.5
AD 11	86	M	3.8
AD 12	87	M	6
Mean ± S.D.	78.5 ± 5.03		3.17 ± 1.33

Immunoprecipitation and Proteolysis Assay—AD and control brains were homogenized to 10% (w/v) final concentrations in cold buffer containing 50 mM sodium citrate, pH 5.5, 0.1 M NaCl, 1 mM EDTA, and 2 mM β-mercaptoethanol. The homogenate was subjected to three cycles of freezing and thawing to disrupt organelles, followed by centrifugation at 12,000 $\times$ *g* for 15 min. Protein concentration was determined by modified Lowery, and 150 μg of the 12,000 $\times$ *g* extract was precleared with 45 μl of protein G beads (Pierce) for 4 h. After low speed centrifugation, the beads were kept as a control for nonspecific binding, and the extract was incubated on a rotater with 1.9 μg of anti-human legumain (AEP; 1:500; R & D Systems, Minneapolis, MN) and 45 μl of protein G beads overnight at 4 °C. The sample was centrifuged at low speed, the supernatant contained the immunodepleted fraction, and the beads were used as the IP fraction. To perform the proteolysis assay, 50 ng of either GST-I_2^{PP2A}-WT (wild-type) or GST-I_2^{PP2A}-M (Asn-175 mutated to

Gln) were incubated in the presence of 10 μg of extract, IP, immunodepleted, cytosolic, lysosomal, or nuclear fraction at 30 °C for different times, and the reaction was stopped by boiling the samples in Laemmli buffer; GST-I_2^{PP2A}-WT treated identically but with buffer only served as a control.

Co-immunoprecipitation—Cos-7 cells were transfected with pTRE2hyg/HA-I_2^{PP2A} and lysed by sonication in 10 mM Tris-HCl, pH 7.6, 50 mM NaCl, 1 mM EDTA, 1 mM EGTA, 10 μg/ml aprotonin, and 10 μg/ml pepstatin. The lysate was centrifuged at 12,000 × *g* for 15 min. The supernatant was incubated with anti-legumain (AEP) precoupled onto protein G-agarose (4 μg of goat anti-AEP/500 μg of cell lysate) overnight at 4 °C. After extensive washing, the bound proteins were eluted from the beads by boiling in Laemmli sample buffer and subjected to Western blot analyses. The IP products were detected with goat anti-AEP (1:200; R & D Systems) and co-IP with mouse anti-HA (1:10,000; Sigma Clone HA-7).

Metabolically Active Rat Brain Slices—The protocol was as described previously (37). Briefly, male Wistar rats (Charles River Lab, Wilmington, MA) 2–3 months old were injected intraperitoneally with 50 mg/kg pentobarbital and decapitated when deeply anesthetized. The brains were immediately removed and cooled down in ice-cold artificial cerebrospinal fluid (aCSF) consisting of 126 mM NaCl, 3.5 mM KCl, 1.2 mM NaH_2PO_4, 1.3 mM $MgCl_2$, 2.0 mM $CaCl_2$, 11 mM D(+)-glucose, 25 mM $NaHCO_3$, pH 7.4 (control), 6.5, or 5.5, for 7–8 min. The hippocampus and surrounding cortex from each brain was dissected and chopped into 400-μm-thick coronal slices with a Camden Vibraslicer (WP Inc., Sarasota, FL). The slices were transferred into a chamber containing the aCSF and incubated at 33 °C for 2 h. The oxygenation of the aCSF was carried out by bubbling the solution with a mixture of 95% O_2 and 5% CO_2 during the entire procedure. At the end of incubation, the brain slices were homogenized with homogenizing buffer (described above) at a ratio of 9 ml of buffer/1.0-g tissue slice. After protein assays, the samples were prepared for SDS-PAGE and subjected to Western blots.

PP2A Activity Assay—PP2A activity was assayed as described previously (38). Briefly, an ELISA was used to assay PP2A activity in 12,000 × *g* extract, of metabolically active rat brain slices. No phosphatase inhibitors were used in the homogenizing buffer for this protocol. A 96-well plate was coated for 8 h at room temperature with 60 μl of coating buffer (35 mM $NaHCO_3$) containing 8.0 μg/ml synthetic Tau phosphopeptide p17 corresponding to Tau amino acid residues 194–207, to which three lysines were added at the C-terminal end (Ac-Arg-Ser-Gly-Tyr-Ser-Ser(OPO_3^{2-})-Pro-Gly-Ser-Pro-Gly-Thr-Pro-Gly-Lys-Lys-Lys-NH_2) to enhance its binding to the microtiter plate. For blocking, the coating solution was removed, and the wells were blocked with 150 μl of protein-free blocking buffer (Pierce) at 4 °C overnight. The plates were then washed two times for 15 min with 150 μl/well 50 mM Tris-HCl, pH 7. The enzymatic reaction was performed with 60 μl/well of 0.15 μg of extract protein in reaction buffer containing 50 mM Tris-HCl, pH 7, 20 mM β-mercaptoethanol, 2 mM EGTA, 2 mM $MnCl_2$, and 0.01 mg/ml BSA in the presence or absence of 20 nM okadaic acid as a specific inhibitor of PP2A. The plates were incubated for 60 min at 30 °C in a moist chamber. To stop the enzyme reaction, the mixture was removed, and the wells were washed two times for 10 min with blocking buffer containing 50 mM NaF and then with the buffer without NaF. Each well was then incubated with 75 μl of the monoclonal antibody Tau-1, which recognizes Tau unphosphorylated at Ser-198/199/202 (1:25000) (39) overnight at 4 °C. The plates were quickly washed three times and two times further for 10 min with 50 mM TBS, 0.05% Tween 20, followed by the same washes with only TBS. The plates were incubated with secondary antibody (peroxidase-linked goat anti-mouse IgG, 1:5000) for 1 h at room temperature. Finally, the plates were washed as indicated previously, and the color reaction was performed using 70 μl of tetramethylbenzidine/well, and the development was monitored for 30 min at 650 nm in a microtiter plate reader. The values of the samples with okadaic acid were subtracted from the corresponding samples without okadaic acid to obtain the PP2A activity.

Western Blots—Western blots were carried out using 10 or 15% SDS-PAGE, PVDF membrane of 0.45 μm pore size and blocking with 5% skim milk. The following primary antibodies were used for the blots: anti-human legumain (AEP) (1:500; R & D Systems), anti-LAMP-2 (1 μg/ml; Santa Cruz Biotechnology, Santa Cruz, CA), mouse anti-I_2^{PP2A} N-term (10E7; 5 μg/ml), anti-c-Myc (1:1000; Sigma-Aldrich), anti-Tau Ser(P)-262/Ser-356 (12E8; 1:500), (40), anti-Tau Thr(P)-205, anti-Tau Ser(P)-214, anti-Tau Thr(P)212, anti-Tau Ser(P)-199 (1:1,000; Biosource, Camarillo, CA), pan Tau antibody, Tau 5 (1:2000; Millipore, Temecula, CA), anti-GAPDH (1:2000; Santa Cruz Biotechnology), anti-β-actin (1:2000; Sigma), and anti-histone 3 (1:1000; Santa Cruz Biotechnology). Immunoblots were probed with the corresponding anti-mouse, anti-rabbit (1:5,000; Jackson Immuno Research), or anti-goat HRP secondary antibodies (1:1000; Invitrogen) and detected using the enhanced chemiluminescence reagents (Thermo Scientific, Rockford, IL). Multigauge V3 software (Fuji Photo Film, Tokyo, Japan) was used to quantify the protein bands in Western blots. Student's *t* test was performed for the statistical analysis between two groups.

Immunohistochemistry and Immunocytochemistry—Immunohistochemical staining of AD and control brain paraffin sections was performed after treatment of the sections for antigen retrieval in microwave for 2 min in citrate buffer that contained 7 mM citric acid and 10 mM sodium citrate (41). The primary antibodies were used at the indicated dilution: anti-histone 3 (1:100), mouse mAb anti-I_2^{PP2A} N-term (10E7; 1:200), rabbit anti-I_2^{PP2A} N-term (1483; 1:200 (32)) anti-Tau Ser(P)-262/Ser-356 (12E8; 1:200), anti-LAMP-2 (1:50), anti-human legumain (AEP; 1:50), anti-HA (1:500; Sigma-Aldrich), and anti-TOPRO 3 (nuclear staining; 1:1000; Invitrogen). The secondary antibodies used were: Alexa 488-conjugated goat anti-rabbit IgG (H+L), Alexa 488-conjugated donkey anti-goat IgG (H+L), Alexa 555-conjugated goat anti-mouse IgG (H+L), Alexa 555-conjugated donkey anti-mouse IgG (H+L), Alexa 555-conjugated goat anti-rabbit IgG (H+L) (1:500; Molecular Probes, Carlsbad, CA), and CY5 goat anti-mouse IgG (H+L) (1:500; Jackson Laboratory). For triple immunostaining, the cells or tissue sections were incubated with secondary antibodies donkey anti-goat for 2 h and then further incubated with goat anti-

mouse to avoid cross-reaction. The sections were subjected to treatment with Sudan Black 0.3% (w/v) in 70% EtOH (v/v) for 10 min to inhibit autofluorescence of lipofuscin. Finally sections were analyzed using confocal microscope Nikon Eclipse 90i, 12 images into 5-μm depth through the *z* axis were scanned, and horizontal z sections were collected and analyzed individually for co-localization and projected as superimposed stacks (merge).

For diaminobenzidine staining, AD and control brain paraffin sections were processed as above except that the sections were treated with 0.5% hydrogen peroxide in PBS (Fisher) for 15 min after the antigen retrieval. The tissue sections were incubated with anti-human legumain (1:100), followed by anti-goat HRP-conjugated secondary antibody (1:250). Thereafter, a solution of 0.01% hydrogen peroxide combined with 0.06% 3,3′-diaminobenzidine (Sigma-Aldrich) in PBS was used to develop the reaction. The samples were counterstained with hematoxylin (Sigma-Aldrich) to visualize the nuclei.

Cell Culture, Plasmids, Transfection, and AEP Knockdown with siRNA—I_{2FL}-Myc was generated by subcloning I_2^{PP2A} into a C-terminal Myc-tagged pcDNA3.1 vector (Invitrogen) as previously described (42). HA-I_{2FL} was generated by subcloning I_2^{PP2A} into an N-terminal HA-tagged pTRE2hyg vector (Clontech). AEP, a homosapien legumain transcript variant 1, purchased from OriGene Technologies, Inc. (Rockville, MD), was cloned into a pCMV6-XL5 vector.

Cos-7 and SH-SY5Y cells (obtained from ATCC, Manassas, VA) were grown in 25-cm^2 flasks at 37 °C with 5% CO_2 in DMEM and advanced DMEM/F-12 medium, respectively, supplemented with 10% fetal bovine serum (Invitrogen); the cells were plated on either 4-well chamber slides for immunocytochemistry or 6-well dishes for Western blots. Cos-7 cells were single- or double-transfected using FuGENE 6 according to the manufacturer's instructions (Roche Applied Science). After 48 h post-transfection, the cells were incubated in pH 5.5 cell culture medium for 30 min as acid condition treatment; then either the cells were fixed with 4% paraformaldehyde in PBS for immunocytochemistry, or the medium was removed and the cells were lysed in lysis buffer (50 mM Tris-HCl, pH 7.4, 150 mM NaCl, 10 mM β-mercaptoethanol, 50 mM sodium fluoride, 1 mM sodium vanadate, 0.1% Triton X-100, 0.1% Nonidet P-40, 0.2% sodium deoxycholate, 2 mM EDTA, 5 mM 4-(2-aminoethyl) benzenesulfonyl fluoride, 10 μg/ml aprotinin, leupeptin, pepstatin). The cells were subjected to either 10% SDS-PAGE for HA-I_2^{PP2A} or 15% SDS-PAGE for I_{2FL}-Myc, followed by Western blots.

To induce AEP knockdown, SH-SY5Y cells were cultured in advanced DMEM F-12 medium and transfected with siRNA against human AEP (siAEP; legumain siRNA(h); Santa Cruz Biotechnology) using Lipofectamine 2000 (Invitrogen) according to the manufacturer's instructions. After 48 h post-transfection, the cells were either lysed in pH 7.4 for control or pH 6.0 lysis buffer (as above, but without pepstatin and phosphatase inhibitors) or treated with 150 μM kainic acid (Tocris Bioscience, Minneapolis, MN) for 24 h (18) and then lysed as above at pH 7.4; SH-SY5Y cells treated identically but without siAEP were used as a control. The cell lysates were subjected to 10% SDS-PAGE, followed by Western blots.

Expression and Purification of Recombinant Wild Type and Mutated I_2^{PP2A}—WT I_2^{PP2A} construct was subcloned into N-terminal GST-tagged pGEX-6P-1 plasmid (GE Healthcare) and transformed into *Escherichia coli* BL21 host strain for expression. A 500-ml culture of *E. coli* harboring pGEX-6P-1/GST-I_2^{PP2A}-WT plasmid was grown at 37 °C to an *A* level of ~600 and induced with 0.4 mM isopropyl β-D-1-thiogalactopyranoside at room temperature for 4 h before harvesting the bacteria by centrifugation. The bacteria were resuspended in 25 ml of cold PBS with protease inhibitor mixture (Sigma-Aldrich) and lysed by sonication and mixed after adding Triton X-100 to 1% final concentration. All purification procedures were carried out at 4 °C. The total soluble fraction was recovered by centrifugation at 8500 × *g* for 10 min. DTT was added to the extract to a final concentration of 5 mM, followed by incubation for 4 h with 5 ml of glutathione-Sepharose beads. The beads were then transferred to a disposable column and washed with PBS. The GST-I_2^{PP2A} was then eluted from the beads with 10 mM GSH in 50 mM Tris HCl, pH 8.5. The eluted protein was dialyzed and stored in aliquots at −80 °C. Mutant I_2^{PP2A} (I_2^{PP2A}-M) was constructed by PCR amplification from wild type I_2^{PP2A} as a template. The mutation was generated by amplifying individual fragments that contain the mutated region replacing Asn-175 for Gln using the following primers: forward, 5′-CGT TCG AGT CAA ACG CAG CAA AAA GCC AGC AGG AAG AGG-3′; and reverse, 5′-CCT CTT CCT GCT GGC TTT TTG CTG CGT TTG ACT CGA ACG-3′, and the sequences were flanked by BamHI and EcoRI for insertion into pGEX-6P-1 plasmid vector with the following primers: forward, 5′-CG GGA TCC ATG TCG GCG CCG GCG GCC AAA GTC AGT AAA AAG-3′; and reverse, 5′-CG GAA TTC CTA GTC ATC TTC TCC TTC ATC CTC CTC TCC-3′. The expression and purification of pGEX-6P-1/GST-I_2^{PP2A}-M was carried out using the same protocol as above for the wild type fusion protein.

RESULTS

Activation of AEP and Cleavage of I_2^{PP2A} Are Increased in AD Brain—To determine the possible involvement of AEP in the cleavage of I_2^{PP2A}, we analyzed frontal cortex homogenates from eight AD and ten non-AD control cases for levels of activated AEP and the cleaved I_2^{PP2A} by Western blots. We found that the level of the 36-kDa active AEP was higher in AD than control brains (Fig. 1*A*), and the level of pro-AEP (56 kDa) was lower in AD than in control cases (Fig. 1*B*). The level of I_{2NTF}, a product of I_2^{PP2A} cleavage by AEP, was found to be increased in AD as compared with control cases. These data raised the possibility of the involvement of AEP in the cleavage of I_2^{PP2A}.

To learn whether activated AEP cleaves I_2^{PP2A}, we investigated the interaction between the two proteins as follows. We transfected Cos-7 cells with PTRE2hyg/HA-I_2^{PP2A} and then immunoprecipitated AEP with anti-legumain (AEP). We found that I_2^{PP2A} co-immunoprecipitated with activated AEP (Fig. 1*C*), suggesting an interaction between the two proteins.

Translocation of AEP and I_2^{PP2A} to Cytoplasm Is Increased in AD Brain—Because AEP and I_2^{PP2A} are lysosomal and nuclear proteins, respectively, we evaluated whether there is an interaction between these two proteins and determined in which

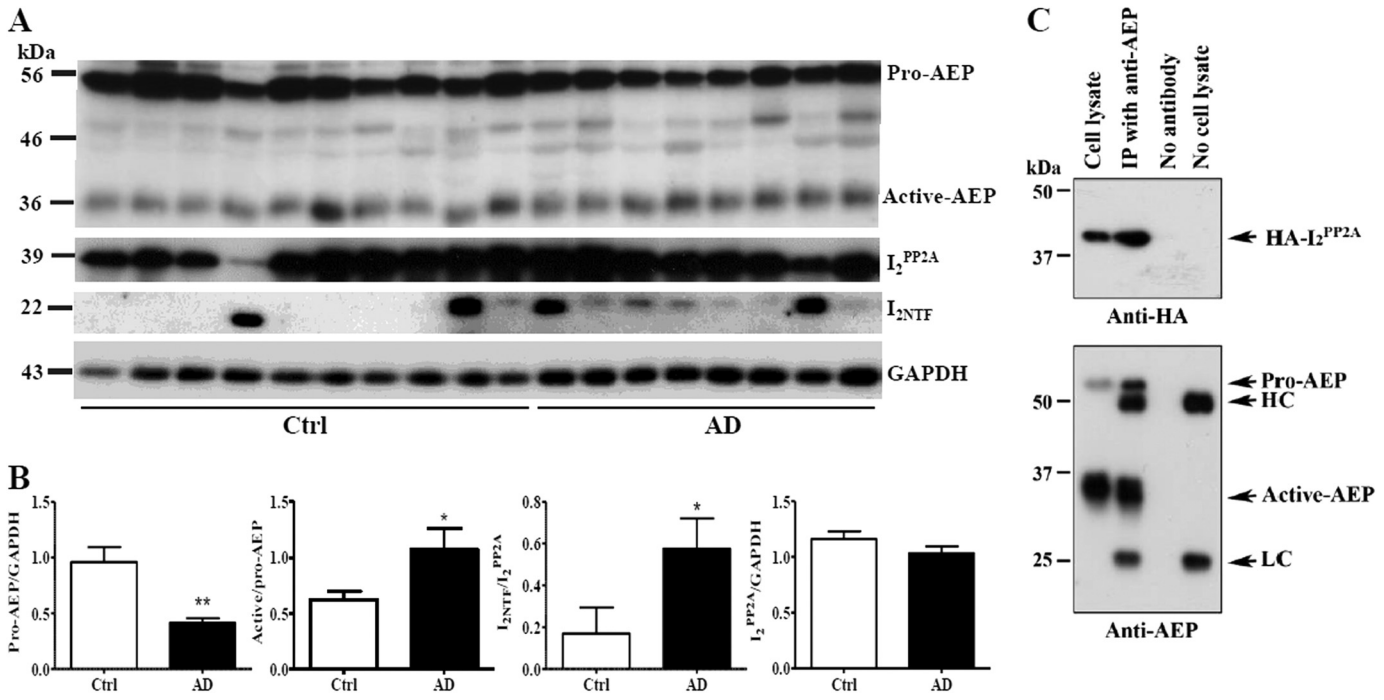

FIGURE 1. **AEP interacts with I_2^{PP2A} and in AD brain the levels of activated AEP and I_{2NTF} are selectively increased.** *A*, AD and control (*Ctrl*) human brain homogenates were subjected to Western blots developed with antibodies to AEP and I_{2NTF}. In AD brain, increases in the levels of both activated AEP (36-kDa band) and I_2^{PP2A} cleavage product I_{2NTF} were found. *B*, quantitation of Western blots showed a decrease in the level of pro-AEP and an increase in the activation of AEP and the cleavage of I_2^{PP2A} into I_{2NTF} in AD brains. *C*, immunoprecipitation of AEP with anti-AEP (legumain) showed co-immunoprecipitation of I_2^{PP2A} from lysates of Cos-7 cells transfected with HA-I_2^{PP2A}.

subcellular compartment this interaction could take place. To identify the location of these proteins, we performed immunohistofluorescence, followed by confocal microscopy on paraffin sections of the hippocampus from AD and control brains. We found increased I_2^{PP2A} cytoplasmic staining in AD relative to control brains (Fig. 2*A*), and the co-localization between I_2^{PP2A} and the nuclear protein histone 3 was higher in control than in AD brains. Using LAMP-2 as a lysosomal marker, we observed a low level of co-localization between lysosomes and AEP in AD brains; the AEP staining was mainly cytoplasmic and diffuse, and the LAMP-2 staining showed vesicle formations that were larger than normal lysosomes. In contrast, we observed a high level of co-localization between LAMP-2 and AEP, as well as increased number and definition of the lysosomal structures in control cases (Fig. 2*B*). These data suggest that both AEP and I_2^{PP2A} undergo translocation respectively from lysosomes and nucleus to cytoplasm and that the interaction between these proteins probably takes place mainly in this compartment in AD brain.

AEP Is Translocated from Neuronal Lysosomes to Cytoplasm and Co-exists with I_2^{PP2A} and Abnormally Hyperphosphorylated Tau in AD—I_2^{PP2A} was previously shown to undergo cleavage into I_{2NTF} and I_{2CTF} and translocate from the neuronal nucleus to the cytoplasm in AD brain (32). However, translocation of AEP from lysosome to cytosol was not understood. To address this question, we studied the level of active AEP in subcellular fractions from AD and control brains. We used LAMP-2 to distinguish lysosomal from nonlysosomal fractions (Fig. 3). Western blot analysis by densitometry showed that active AEP is mostly concentrated in the cytosol more in AD than control brains (Fig. 3, *A* and *B*). Consistent with these data, immunohistochemical staining of AD brain with anti-AEP showed a marked signal in the neuronal cytoplasm along with lysosomes and a weaker reaction in the nucleus (Fig. 3*D*, *right inset*); the tangle-bearing neurons showed especially robust cytoplasmic immunostaining (Fig. 3*D*, *left inset*). The level of active AEP in the nuclear fraction showed a small increase in AD as compared with control brains, but this increase was not significant (Fig. 3*C*).

Because it is already known that I_2^{PP2A} plays an important role in Tau hyperphosphorylation (38), we evaluated whether the cytosolic distribution of AEP is associated with hyperphosphorylated Tau in AD brain. For this purpose, hippocampal sections were subjected to triple staining with anti-AEP, anti-I_2^{PP2A}, and anti-pTau. The analysis of these data by confocal microscopy revealed that cells without Tau pathology had AEP immunostaining in lysosomes (Fig. 3*E*, *arrow*, punctated staining), whereas hyperphosphorylated Tau-positive neurons showed diffuse AEP staining in the cytoplasm (Fig. 3*E*, *arrowhead*). Moreover, I_2^{PP2A} cytoplasmic staining was found in hyperphosphorylated Tau-bearing neurons. These data suggest that translocation of AEP from neuronal lysosomes to cytoplasm could be involved in Tau pathology in AD.

AEP from the Cytosolic Fraction of AD Brain Cleaves Recombinant I_2^{PP2A}—The above findings suggested that in AD, I_2^{PP2A} and AEP are released to the cytoplasm where these proteins can interact and I_2^{PP2A} can be cleaved by AEP. However, there is a possibility that an enzyme other than AEP could also be responsible for this cleavage under the same conditions. Because previous reports indicated that the cleavage of I_2^{PP2A} occurs at Asn-175 (18, 32), first we investigated whether the proteolytic activity from AD brain is able to cleave I_2^{PP2A} at Asn-175 to

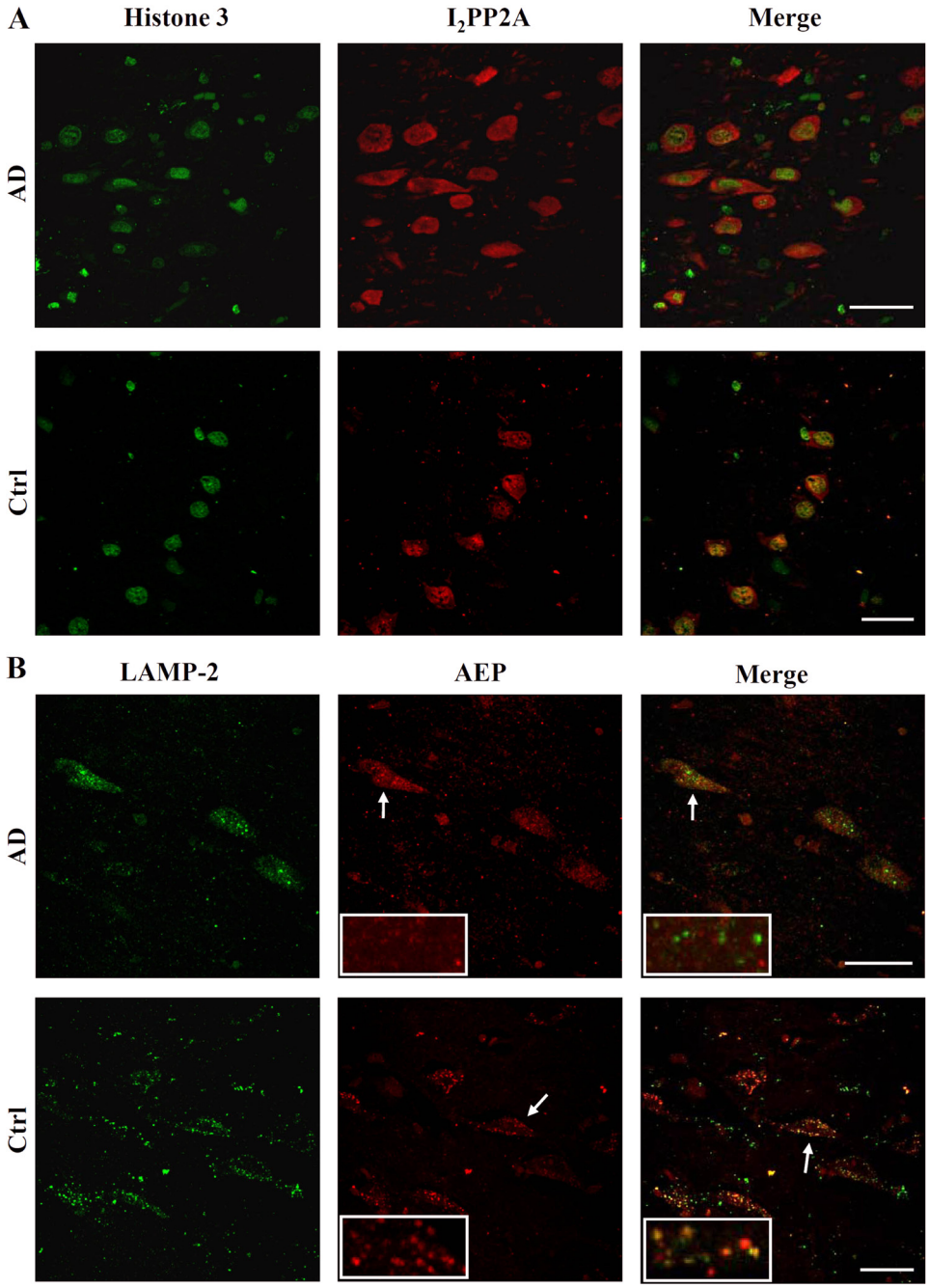

FIGURE 2. **I_2^{PP2A} and AEP are localized mainly in neuronal cytoplasm in AD brain.** *A*, AD and control (*Ctrl*) hippocampal paraffin sections were subjected to double immunostaining with anti-histone 3 (a nuclear marker) and anti-I_2^{PP2A} and analyzed by laser scanning confocal microscopy. In AD brains, I_2^{PP2A} was localized mainly in neuronal cytoplasm, whereas in control cases it was seen in the nucleus. *B*, immunostaining with anti-LAMP-2 (a lysosomal marker) and anti-AEP showed a diffuse staining of AEP in neuronal cytoplasm in AD and lysosomal localization in control brain neurons. The *insets* show high magnification of the area indicated by the *arrow*. *Scale bar*, 40 μm.

generate I_{2NTF}. Second, we determined whether AEP is the enzyme responsible for this cleavage. Third, we investigated in which subcellular compartment this cleavage takes place. To address these questions, we purified GST-I_2^{PP2A} recombinant fusion protein and subjected it to proteolysis with AD brain extract. GST-I_2^{PP2A} was cleaved in a time-dependent manner generating I_{2NTF} (Fig. 4*A*). To confirm that this cleavage was catalyzed by AEP, we mutated Asn-175 of I_2^{PP2A} to Gln in GST-I_2^{PP2A} and studied its proteolysis with brain extract. We found that wild type GST-I_2^{PP2A} but not the mutated GST-I_2^{PP2A} was cleaved when treated with the brain extract (Fig. 4*B*). To verify that only AEP in the brain extract was responsible for the cleavage of I_2^{PP2A} at Asn-175, we IP AEP from AD brain extract and performed the proteolysis assay as above. GST-I_2^{PP2A} was cleaved by IP-AEP but not by AEP immunodepleted brain extract (Fig. 4*C*). Because, as described above, we observed that both I_2^{PP2A} and active AEP were located in the cytosol from AD brain, we evaluated where in the cell I_2^{PP2A} cleavage could take place. After subcellular fractionation of the brain, GST-I_2^{PP2A} was subjected to proteolysis by cytosolic, lysosomal, and

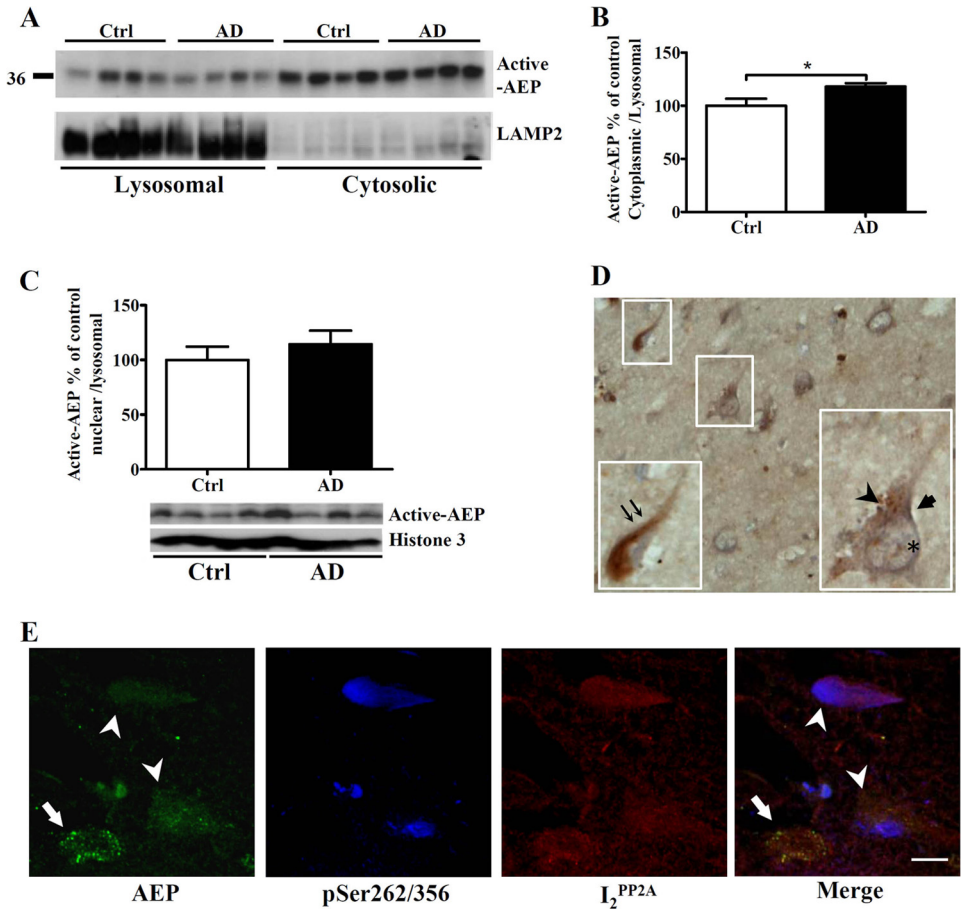

FIGURE 3. **Active AEP is selectively translocated from neuronal lysosomes to the cytoplasm and the nucleus and is associated with abnormally hyperphosphorylated Tau in AD.** *A*, AD and control (*Ctrl*) human brain samples were subjected to subcellular fractionation, followed by Western blots to determine the distribution of AEP. *B*, the translocation of active AEP from the neuronal lysosomes to the cytoplasm was found. LAMP-2 was used as specific marker for lysosomal fraction. *C*, Western blot analysis showed a trend but no significant increase in translocation of active AEP from neuronal lysosomes to the nucleus in AD brain. *D*, immunohistochemical staining of AEP in AD hippocampal paraffin sections counterstained with hematoxylin showed its localization in neuronal lysosomes (*arrowhead*), cytoplasm (*arrow*), nuclei (*asterisk*), and neurofibrillary tangles (*double arrows*). *E*, AD and control hippocampal paraffin sections were subjected to triple immunohistofluorescent staining with anti-AEP, anti-I_2^{PP2A}, and anti-Ser(P)-262/356 (12E8) Tau and analyzed by laser scanning confocal microscopy. Diffuse cytosolic staining of AEP was observed in Tau pathology-bearing neurons (*arrowheads*), whereas in cells without hyperphosphorylated Tau AEP was localized in lysosomes (*arrow*). *Scale bar*, 10 μm.

nuclear fractions. The cytosolic fraction showed the highest concentration of the active AEP and was most effective in cleaving I_2^{PP2A}, generating I_{2NTF} (Fig. 4, *D–F*). Neither the lysosomal fraction nor the nuclear fraction showed any significant cleavage of I_2^{PP2A} (Fig. 4*D*). These data suggested that AEP is most likely the primary enzyme in the brain that cleaves I_2^{PP2A} at Asn-175, and this cleavage takes place mainly in the neuronal cytoplasm in AD.

I_2^{PP2A} Co-localizes with AEP in the Cytoplasm of Cos-7 Cells and Produces Both I_{2NTF} and I_{2CTF} under Acidic Conditions—AEP is a lysosomal zymogen that undergoes autoproteolysis in acidic conditions during activation. We found that this enzyme is responsible for I_2^{PP2A} cleavage, but the generation of I_{2NTF} and I_{2CTF} fragments, both of which have been reported to inhibit (33), was not established. To confirm the generation of both I_{2NTF} and I_{2CTF} from the cleavage of I_2^{PP2A} by AEP, we incubated Cos-7 cells after 48 h of double transfection with HA-I_2^{PP2A} and AEP in acidic medium, pH 5.5, for 30 min, followed by immunocytochemistry with anti-HA and anti-AEP. In normal medium-treated cells (control), I_2^{PP2A} was located in the nucleus and co-localized with the nuclear marker TOPRO 3, and AEP staining had a vesicular appearance in the cytoplasm indicating lysosomal location. However, after incubation in acidic medium, both I_2^{PP2A} and AEP were localized diffused in the cytoplasm (Fig. 5*A*). To determine whether I_{2NTF} and I_{2CTF} were formed under acidic conditions, Cos-7 cells were either co-transfected or individually transfected with AEP and I_2^{PP2A}-Myc. I_{2CTF} was detected using anti-Myc, whereas I_{2NTF} was recognized by 10E7 antibody. We evaluated the levels of transfections and observed an increase in active AEP in AEP transfected cells, particularly under acidic conditions (Fig. 5*B*). I_2^{PP2A} was cleaved in the double-transfected cells generating two protein bands at 22 and 24 kDa (Fig. 5*C*). The band at 24 kDa, a larger N-terminal cleavage product than I_{2NTF}, was also present in the I_2^{PP2A} singly transfected cells, but this band and the 39-kDa band disappeared, whereas only 22-kDa I_{2NTF} was seen in double-transfected cells under acidic condition (Fig. 5*C*, *upper panel*). The cleavage of I_2^{PP2A} by AEP in the double-transfected cells showed the appearance of a 17-kDa I_{2CTF} fragment under acidic conditions (Fig. 5*C*, *lower panel*). These data suggest that I_2^{PP2A} and AEP translocation to the cytoplasm requires acidic conditions to generate both I_{2NTF} and I_{2CTF} fragments.

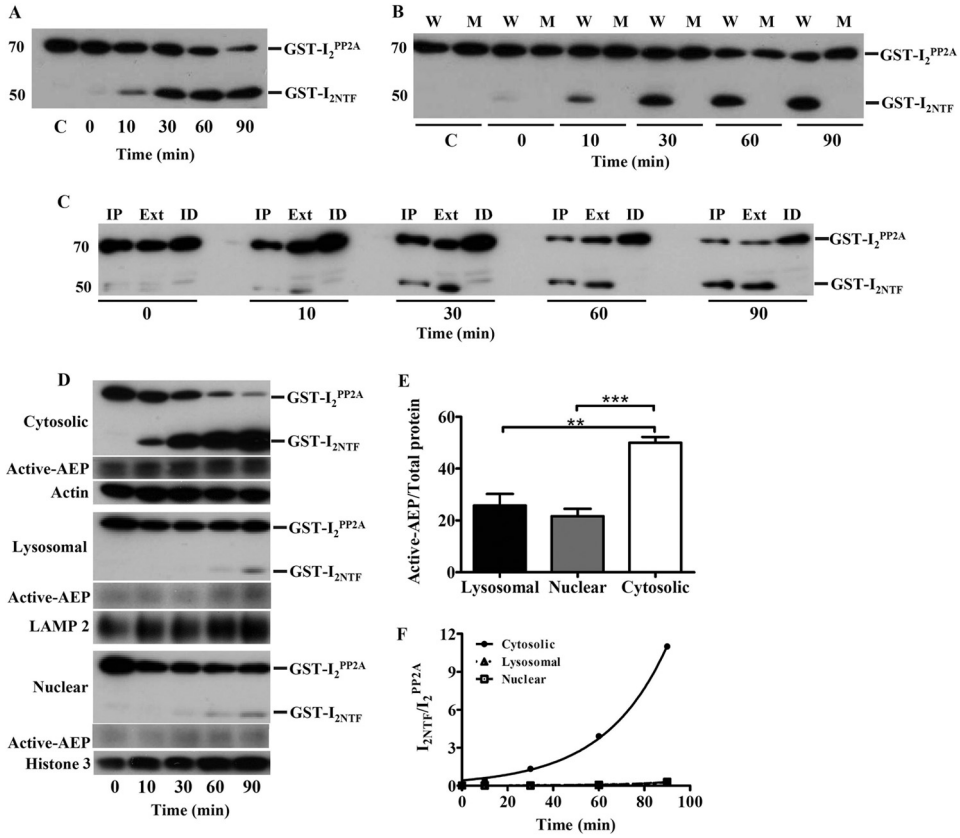

FIGURE 4. **GST-I_2^{PP2A} is cleaved by AEP from the cytosolic fraction of AD brain.** *A*, GST-I_2^{PP2A} recombinant fusion protein was cleaved by AD brain extract (*Ext*) in a proteolysis assay, generating GST-I_{2NTF} in a time-dependent manner. *B*, GST-I_2^{PP2A} (*W*) but not mutated N175Q (*M*) GST-I_2^{PP2A} could be cleaved with the brain extract. *C*, under the same proteolysis conditions GST-I_2^{PP2A} was cleaved by the IP AEP, but not by the immunodepleted extract (*ID*). *D*, the cytosolic fraction isolated from AD brains was markedly more robust than the lysosomal or the nuclear fraction in cleavage of GST-I_2^{PP2A} into GST-I_{2NTF} during 0–90 min of incubation. *E* and *F*, quantitation of Western blots showed that the level of active AEP was the highest in the cytosolic fraction (*E*) and that GST-I_2^{PP2A} was most robustly cleaved by the cytosolic fraction (*F*). Actin, LAMP-2, and histone 3 were used as specific markers of cytoplasm, lysosomes, and nuclei, respectively.

Treatment of Metabolically Active Rat Hippocampal Slices in Acidic Conditions Leads to Activation of AEP, Cleavage of I_2^{PP2A}, Inhibition of PP2A, and Hyperphosphorylation of Tau—AEP activation has been previously reported in a stroke mouse model (18), which indicates that acidic conditions could play an important role for AEP activity, and we postulated that Tau hyperphosphorylation increases as a consequence of this activation. To assess this relation, we incubated metabolically active rat hippocampal slices in aCSF of different pH levels. After incubation, to evaluate AEP activation (36-kDa fragment) and Tau hyperphosphorylation, the tissue slices were lysed and used for Western blots and PP2A activity assays (Fig. 6). Densitometric analysis of the blots showed an increase in AEP activation (Fig. 6*B*) and, because of cleavage of I_2^{PP2A}, a reduction in the level of I_{2FL} at acidic pH (Fig. 6*C*). Corresponding to the cleavage of I_2^{PP2A} at acidic conditions, the PP2A activity was inhibited (Fig. 6*D*), and the abnormal hyperphosphorylation of Tau was increased at several sites (Fig. 6*E*). These changes increased with decreasing pH from pH 7.4 to 5.5. These data showed a clear pH dependence from neutral to acidic pH in activation of AEP and consequent cleavage of I_2^{PP2A}, a decrease in PP2A activity, and an increase in the abnormal hyperphosphorylation of Tau.

Abnormal Hyperphosphorylation of Tau Produced by Acidic Conditions Is Caused by the Activation of AEP—To learn whether the abnormal hyperphosphorylation of Tau produced during acidosis of the brain as in ischemia could be due to the activation of AEP, we treated the SH-SY5Y cells with siRNA to human AEP, followed by treatment with kainic acid or acidic pH. Transfection of SH-SY5Y cells with the siRNA successfully knocked down the expression of the active AEP; the level of the abnormal hyperphosphorylation of Tau at Ser-262/356 in cells treated with kainic acid was markedly increased as compared with the identically treated cells with siAEP or cells treated with neither siRNA nor kainic acid as a control (Fig. 6*F*). Furthermore, although pH 6.0 treatment increased the abnormal hyperphosphorylation of Tau at Ser-262/356, no such differences were seen between AEP knocked down SH-SY5Y cells lysed at pH 6.0 and the control treated cells lysed at the neutral pH (Fig. 6*G*).

DISCUSSION

AD is a multifactorial disease that involves several etiopathogenic mechanisms (43). Neurofibrillary pathology of hyperphosphorylated Tau is a histopathological hallmark of AD and related neurodegenerative disorders called tauopathies. Different factors are involved in the onset of this pathology, and the origin of the sporadic forms of these diseases remains unclear. However, a key mechanism that leads to neurofibrillary pathology is the abnormal hyperphosphorylation of Tau (39, 45). In the present study, we evaluated a target that is upstream of Tau hyperphosphorylation in AD. We found that: (i) AEP, which

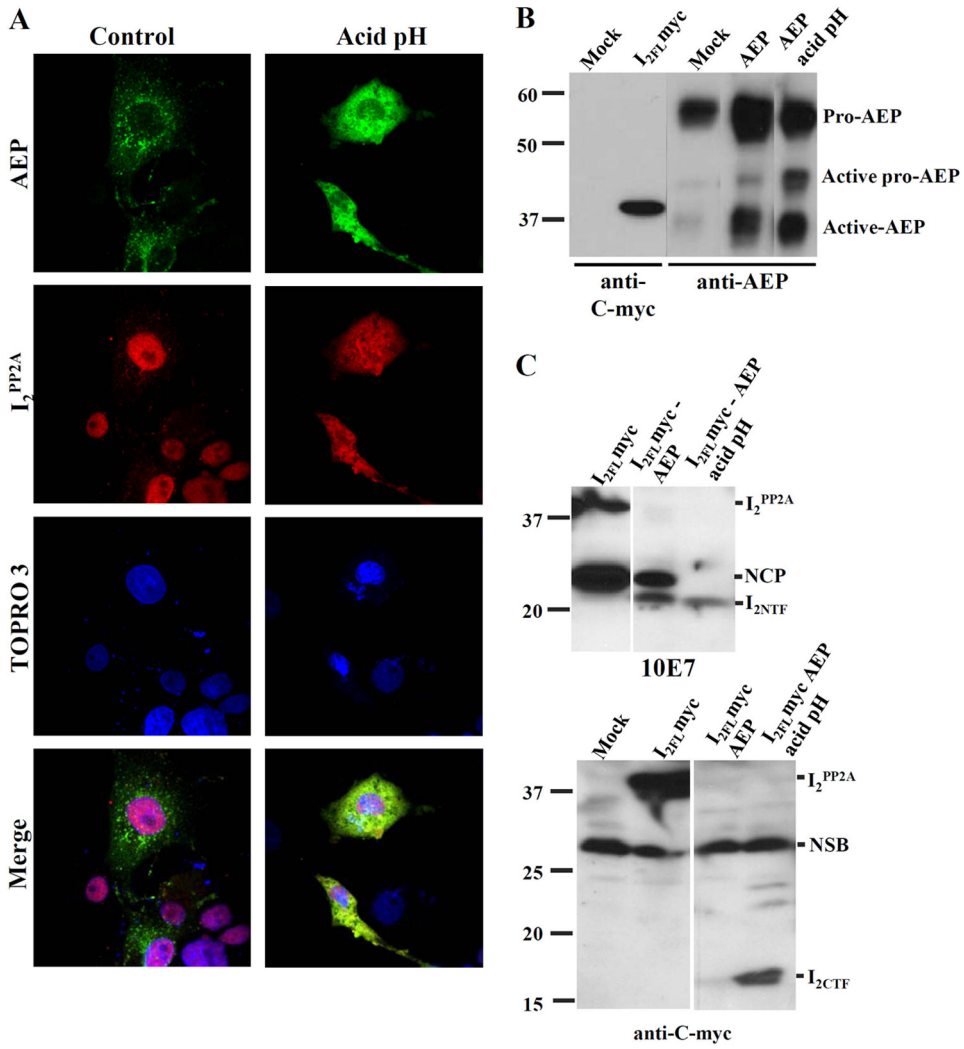

FIGURE 5. **I_2^{PP2A} is released from the cell nucleus to the cytoplasm, co-localized with AEP and cleaved into I_{2NTF} and I_{2CTF} under acidic conditions.** *A*, Cos-7 cells co-transfected with AEP and HA-I_2^{PP2A} were subjected to immunocytochemical staining with anti-AEP and anti-HA, respectively. I_2^{PP2A} was seen mostly localized in the nucleus in Cos-7 cells but translocated to the cytoplasm following incubation with acid pH medium, pH 5.5, for 30 min. Under the acidic condition, AEP was seen diffused into cell cytoplasm and the nucleus. *B*, protein expressions evaluated by Western blots. Cos-7 cells were either co-transfected or individually transfected with AEP and I_2^{PP2A}-Myc and incubated with neutral pH or acid pH medium for 30 min. At acid pH, the active pro-AEP and active AEP signals were markedly increased. *C*, in the same conditions as in *B*, cells were lysed, followed by Western blots developed with anti-I_{2NTF} (10E7) or anti-I_{2CTF} (anti-c-Myc). In the presence of acidic conditions, cells co-transfected with AEP and I_{2FL} showed the generation of both I_{2NTF} and I_{2CTF}. *NCP*, N-terminal cleavage product of I_2^{PP2A} that neither requires AEP nor acidic pH; *NSB*, nonspecific band.

cleaves I_2^{PP2A} at Asn-175 into I_{2NTF} and I_{2CTF}, is selectively activated and translocated from the neuronal lysosomes to the cytoplasm and at a much smaller level to the nucleus in AD brain; (ii) AEP cleaves I_2^{PP2A} mainly in the neuronal cytoplasm; and (iii) acidic conditions such as caused by ischemia promote the activation and translocation of AEP as well as the cleavage and the translocation of I_2^{PP2A} to the neuronal cytoplasm and consequently inhibition of PP2A and the abnormal hyperphosphorylation of Tau.

AEP expression and activity have been linked to a number of pathological conditions including atherosclerosis, cancer, and inflammation (11, 12). However, its biological role in these pathologies remains obscure. Here we found that active AEP is present in AD brain at a significantly higher level as compared with control brain. This finding is notable because this is the first study describing AEP involvement in AD pathology. The activation of AEP has been reported in experimental stroke and after transient middle cerebral artery occlusion in mice (18, 19). Stroke elicits acidosis (47), and ischemic lesions (silent strokes) and acidic pH have been described in AD (2, 4). Most lysosomal enzymes are synthesized as zymogens and can be autoactivated under acidic conditions, and it has been demonstrated that AEP requires acidic pH for its activation (9, 48). In the present study, we found that active AEP is selectively translocated from the neuronal lysosomes to the cytoplasm in AD. Previous studies reported that AEP is synthesized in the endoplasmic reticulum as pro-AEP (56 kDa) and is routed via Golgi to the lysosomal system for processing. For this to happen, a pH-reduced environment is crucial (48). In AD brain, the pH is reduced (2). The present study shows that the acidic environment induces AEP activation. The presence of high level of pro-AEP found in control brains in the present study suggests its normal main storage in compartments other than lysosomes such as endoplasmic reticulum. An increase in the cleavage and translocation of

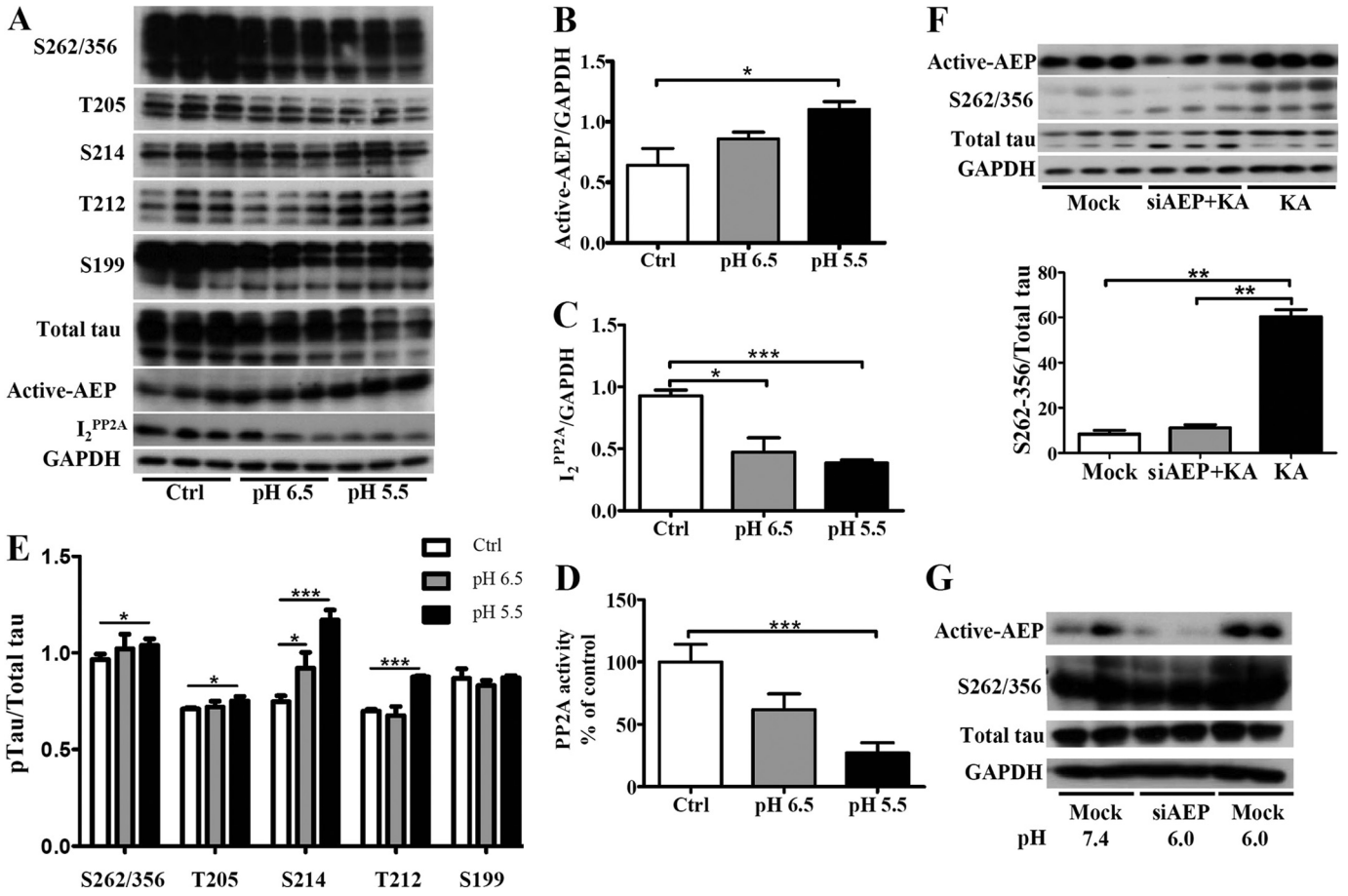

FIGURE 6. **Acidic conditions induce AEP activation, cleavage of I_2^{PP2A}, inhibition of PP2A activity, and Tau hyperphosphorylation.** *A*, rat hippocampal slices after incubation in oxygenated aCSF at three different pH conditions (control, pH 7.4) were subjected to Western blots developed with anti-phospho-Tau and anti-AEP. The blots were analyzed by densitometry. *B–E*, acidic conditions caused an increase in the level of activated AEP (*B*), a decrease in the level of full-length I_2^{PP2A} (*C*), inhibition of PP2A activity (*D*), and increase in abnormal hyperphosphorylation of Tau at Ser-262/356, Thr-205, Ser-214, and Thr-212, but not at Ser-199 (*E*). *F* and *G*, Western blots from SH-SY5Y cells either transfected with AEP-siRNA or reagents alone (mock), treated with kainic acid and then lysed. *F*, knockdown of AEP by siRNA inhibited Tau hyperphosphorylation induced by kainic acid treatment of cells lysed at neutral pH. *G*, knockdown of AEP by siRNA inhibited hyperphosphorylation of Tau seen in cells lysed at pH 6.0.

I_2^{PP2A} in AD brain shown by us previously (32) is consistent with an increase in the level and translocation to neuronal cytoplasm of the activated AEP we found in the present study. In agreement with the present study, I_2^{PP2A} was previously reported to be selectively cleaved at Asn-175 in wild type, but not in AEP null mice (18).

A selective increase in the cleavage and translocation of I_2^{PP2A} from the neuronal nucleus to the cytoplasm in AD brain found in the present study is in agreement with similar findings reported by us previously (32). Although I_2^{PP2A} has been previously reported to translocate to cytoplasm under steady-state conditions in an apparently random fashion (27), during cell migration (26) and under oxidative stress, the marked translocation from the neuronal nucleus to the cytoplasm in AD brain observed in the present study is probably mainly due to its cleavage into I_{2NTF} and I_{2CTF}; the cleavage products I_{2NTF}, a 175-amino acid-long fragment, and I_{2CTF}, a 102-amino acid-long fragment, because of their small sizes, can easily diffuse between the nucleus and the cytoplasm.

The immunohistochemical staining showed that although AEP was primarily co-localized with LAMP-2 in the lysosomal compartment in control brain neurons, it was found diffused in the neuronal cytoplasm in AD brains. Consistent with these findings, pro-AEP is known to be located in different compartments such as endoplasmic reticulum, Golgi, or endosomes (9) before the activation in the lysosomes (48). Furthermore, in kidney, AEP was previously shown to be co-localized with LAMP-2, suggesting its association with late endosomes (17).

We confirmed the translocation of AEP to the neuronal cytoplasm in AD brain by subcellular fractionation. We found that active AEP was located in the lysosomes as well as the cytosol, indicating that in AD, the pathological conditions are favorable in inducing translocation of AEP to the cell cytoplasm. The lysosomal system has been implicated in AD pathogenesis in which multiple alterations in neurons of AD patients were found (49). Lysosomal membrane permeability was previously reported in AD and was speculated to be induced by different factors such as the presence of Aβ (50) or oxidative stress (51). Thus, it is possible that in AD the damage to the lysosomes induces lysosomal membrane permeability, and thereby active AEP is released into the cytosol, where I_2^{PP2A} is also located and could be cleaved by this endopeptidase. In the present study, we observed that neurons with AEP punctate staining did not show Tau hyperphosphorylation in AD brain. However, when AEP was

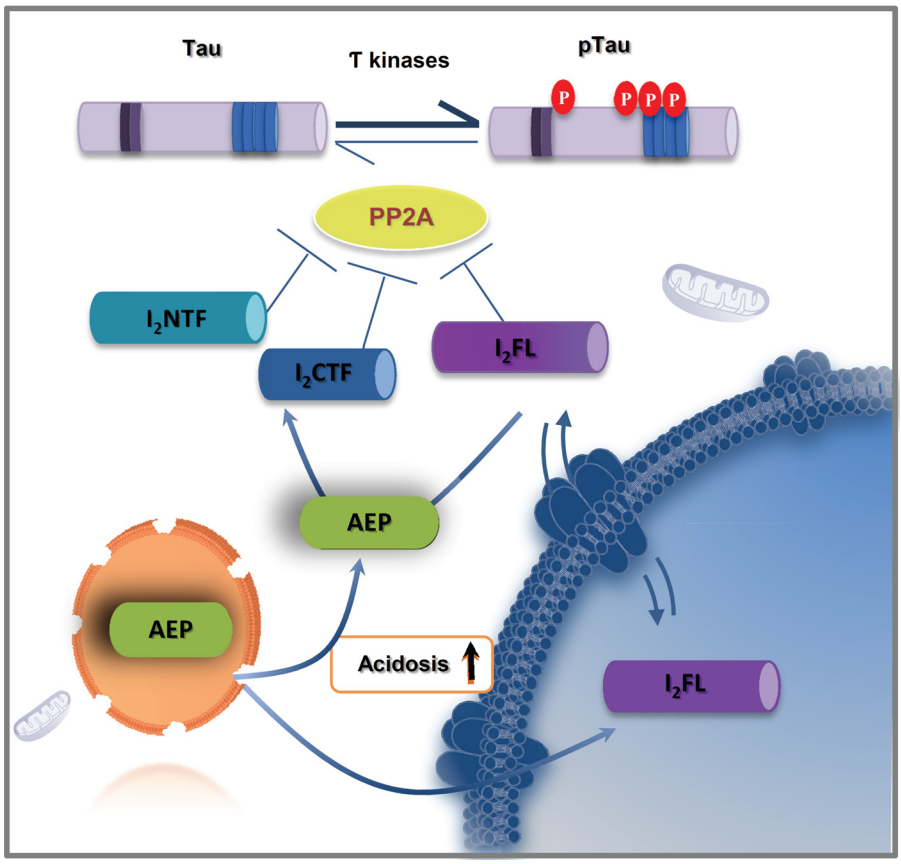

FIGURE 7. **Proposed mechanism of I_2^{PP2A} cleavage and abnormal hyperphosphorylation of Tau by activated AEP in AD.** In AD different etiopathogenic mechanisms activate the translocation of active AEP from the neuronal lysosomes to the cytoplasm and the nucleus where it interacts with I_2^{PP2A} and cleaves it into I_{2NTF} and I_{2CTF}, which bind to PP2A and inhibit its activity. The inhibition of PP2A leads to abnormal hyperphosphorylation of Tau.

found diffused in the cytoplasm, Tau hyperphosphorylation was present, suggesting that the location of cytoplasmic AEP could play an important role in Tau hyperphosphorylation.

The possible mechanism involved is I_2^{PP2A} cleavage by activated AEP, followed by PP2A inhibition by I_{2NTF} and I_{2CTF} and Tau hyperphosphorylation (Fig. 7). This proposed mechanism is supported by the findings that: (i) AEP cleaved I_2^{PP2A} into I_{2NTF} and $I_{2CTF;}$ (ii) AEP in the brain caused this cleavage; (iii) the brain level of activated AEP was increased in AD; (iv) AEP was mainly in the cytosolic fraction; and (v) neurons in which AEP was found diffused in the cytoplasm showed hyperphosphorylated Tau, whereas in neurons in which AEP was mainly localized in lysosomes, Tau was not hyperphosphorylated. The knockdown of AEP with siRNA, followed by acidosis of the SH-SY5Y cells by treatment with kainic acid or acid pH medium, confirmed the role of AEP and the molecular pathway by which acidosis of the brain could lead to Tau pathology.

In mammalian brain PP2A and PP1 account for ~70 and 10% of the total Tau phosphatase activity, respectively (21). Although I_2^{PP2A} inhibits PP2A (20, 52), it activates PP1 (53). Thus, the abnormal hyperphosphorylation of Tau observed in rat hippocampal slices at acidic pH in the present study is most likely primarily due to the inhibition of PP2A caused by activation of AEP and the consequent cleavage of I_2^{PP2A} into I_{2NTF} and I_{2CTF}. The attenuation of the abnormal hyperphosphorylation of Tau by siAEP and at acid pH or kainic acid treatment in SY5Y cells is most likely through inhibition of activation of AEP and consequent reduction of I_2^{PP2A} cleavage and of inhibition of PP2A activity; kainic acid is not a direct PP2A inhibitor. The abnormal hyperphosphorylation of Tau is known to lead to its aggregation into paired helical filaments (45), and our previous studies (34, 35) showed that the expression of I_{2NTF} and I_{2CTF} causes abnormal hyperphosphorylation and aggregation of Tau, as well as neurodegeneration and cognitive impairment in rats.

It is known that lysosomal hydrolase activation requires an optimal acidic pH, but it is not known how AEP is able to function in the cytosol. However, *in vitro* studies have shown that some lysosomal proteases can function at neutral pH (54, 55), confirming their potential for activation outside the lysosomes. Acidic conditions in AD brains increase the lysosomal protease activity and lysosomal membrane permeability (51, 55). Lysosomal enzyme activity in the cytosol has been previously described, such as cytosolic cathepsins in both pathological (56, 57) and physiological (44) apoptotic mechanisms. AEP is predominantly localized in lysosomes but is overexpressed in many types of tumors and associated with enhanced tissue invasion and metastasis. In these cases, AEP can also be found on the cell surface, co-localized with integrin β1 (11), and in blastocysts displaying a pro-survival role (14), indicating that lysosomal location of AEP is not required for its activity. We observed in cultured cells under acidic conditions that both I_2^{PP2A} and AEP translocated to the cytosol. However, the cell morphology and nuclear condensation indicate that these cells undergo patho-

logical states, which could be due to impairment in lysosomal stability caused by acidic conditions in cell culture, as previously reported (46).

It is known that PP2A plays an important role in AD (24). The acidosis associated with ischemic changes could cause PP2A inhibition through activation of AEP and consequent cleavage and translocation of I_2^{PP2A} from the neuronal nucleus to the cytoplasm in AD. AEP could be considered an important trigger and hence a therapeutic target for sporadic AD and related conditions characterized by Tau pathology.

Acknowledgments—We thank Dr. Mohammad Arif for advice on the use of metabolically active brain slices, Dr. George Merz for advice on the confocal microscopy, and Janet Murphy for secretarial assistance.

REFERENCES

1. Cataldo, A. M., Paskevich, P. A., Kominami, E., and Nixon, R. A. (1991) Lysosomal hydrolases of different classes are abnormally distributed in brains of patients with Alzheimer disease. *Proc. Natl. Acad. Sci. U.S.A.* **88,** 10998–11002
2. Yates, C. M., Butterworth, J., Tennant, M. C., and Gordon, A. (1990) Enzyme activities in relation to pH and lactate in postmortem brain in Alzheimer-type and other dementias. *J. Neurochem.* **55,** 1624–1630
3. Cataldo, A. M., Thayer, C. Y., Bird, E. D., Wheelock, T. R., and Nixon, R. A. (1990) Lysosomal proteinase antigens are prominently localized within senile plaques of Alzheimer's disease. Evidence for a neuronal origin. *Brain Res.* **513,** 181–192
4. Pirchl, M., and Humpel, C. (2009) Does acidosis in brain play a role in Alzheimer's disease? *Neuropsychiatrie* **23,** 187–192
5. Bevers, M. B., and Neumar, R. W. (2008) Mechanistic role of calpains in postischemic neurodegeneration. *J. Cereb. Blood Flow Metab.* **28,** 655–673
6. Wen, Y. D., Sheng, R., Zhang, L. S., Han, R., Zhang, X., Zhang, X. D., Han, F., Fukunaga, K., and Qin, Z. H. (2008) Neuronal injury in rat model of permanent focal cerebral ischemia is associated with activation of autophagic and lysosomal pathways. *Autophagy* **4,** 762–769
7. Fang, B., Wang, D., Huang, M., Yu, G., and Li, H. (2010) Hypothesis on the relationship between the change in intracellular pH and incidence of sporadic Alzheimer's disease or vascular dementia. *Int. J. Neurosci.* **120,** 591–595
8. Halfon, S., Patel, S., Vega, F., Zurawski, S., and Zurawski, G. (1998) Autocatalytic activation of human legumain at aspartic acid residues. *FEBS Lett.* **438,** 114–118
9. Li, D. N., Matthews, S. P., Antoniou, A. N., Mazzeo, D., and Watts, C. (2003) Multistep autoactivation of asparaginyl endopeptidase *in vitro* and *in vivo*. *J. Biol. Chem.* **278,** 38980–38990
10. Manoury, B., Hewitt, E. W., Morrice, N., Dando, P. M., Barrett, A. J., and Watts, C. (1998) An asparaginyl endopeptidase processes a microbial antigen for class II MHC presentation. *Nature* **396,** 695–699
11. Liu, C., Sun, C., Huang, H., Janda, K., and Edgington, T. (2003) Overexpression of legumain in tumors is significant for invasion/metastasis and a candidate enzymatic target for prodrug therapy. *Cancer Res.* **63,** 2957–2964
12. Clerin, V., Shih, H. H., Deng, N., Hebert, G., Resmini, C., Shields, K. M., Feldman, J. L., Winkler, A., Albert, L., Maganti, V., Wong, A., Paulsen, J. E., Keith, J. C., Jr., Vlasuk, G. P., and Pittman, D. D. (2008) Expression of the cysteine protease legumain in vascular lesions and functional implications in atherogenesis. *Atherosclerosis* **201,** 53–66
13. Andrade, V., Guerra, M., Jardim, C., Melo, F., Silva, W., Ortega, J. M., Robert, M., Nathanson, M. H., and Leite, F. (2011) Nucleoplasmic calcium regulates cell proliferation through legumain. *J. Hepatol.* **55,** 626–635
14. Wu, B., Yin, J., Texier, C., Roussel, M., and Tan, K. S. (2010) Blastocystis legumain is localized on the cell surface, and specific inhibition of its activity implicates a pro-survival role for the enzyme. *J. Biol. Chem.* **285,** 1790–1798
15. Morita, Y., Araki, H., Sugimoto, T., Takeuchi, K., Yamane, T., Maeda, T., Yamamoto, Y., Nishi, K., Asano, M., Shirahama-Noda, K., Nishimura, M., Uzu, T., Hara-Nishimura, I., Koya, D., Kashiwagi, A., and Ohkubo, I. (2007) Legumain/asparaginyl endopeptidase controls extracellular matrix remodeling through the degradation of fibronectin in mouse renal proximal tubular cells. *FEBS Lett.* **581,** 1417–1424
16. Chen, J. M., Fortunato, M., Stevens, R. A., and Barrett, A. J. (2001) Activation of progelatinase A by mammalian legumain, a recently discovered cysteine proteinase. *Biol. Chem.* **382,** 777–783
17. Shirahama-Noda, K., Yamamoto, A., Sugihara, K., Hashimoto, N., Asano, M., Nishimura, M., and Hara-Nishimura, I. (2003) Biosynthetic processing of cathepsins and lysosomal degradation are abolished in asparaginyl endopeptidase-deficient mice. *J. Biol. Chem.* **278,** 33194–33199
18. Liu, Z., Jang, S. W., Liu, X., Cheng, D., Peng, J., Yepes, M., Li, X. J., Matthews, S., Watts, C., Asano, M., Hara-Nishimura, I., Luo, H. R., and Ye, K. (2008) Neuroprotective actions of PIKE-L by inhibition of SET proteolytic degradation by asparagine endopeptidase. *Mol. Cell* **29,** 665–678
19. Ishizaki, T., Erickson, A., Kuric, E., Shamloo, M., Hara-Nishimura, I., Inácio, A. R., Wieloch, T., and Ruscher, K. (2010) The asparaginyl endopeptidase legumain after experimental stroke. *J. Cereb. Blood Flow Metab.* **30,** 1756–1766
20. Li, M., Makkinje, A., and Damuni, Z. (1996) The myeloid leukemia-associated protein SET is a potent inhibitor of protein phosphatase 2A. *J. Biol. Chem.* **271,** 11059–11062
21. Liu, F., Grundke-Iqbal, I., Iqbal, K., and Gong, C. X. (2005) Contributions of protein phosphatases PP1, PP2A, PP2B and PP5 to the regulation of Tau phosphorylation. *Eur. J. Neurosci.* **22,** 1942–1950
22. Gong, C. X., Singh, T. J., Grundke-Iqbal, I., and Iqbal, K. (1993) Phosphoprotein phosphatase activities in Alzheimer disease brain. *J. Neurochem.* **61,** 921–927
23. Gong, C. X., Shaikh, S., Wang, J. Z., Zaidi, T., Grundke-Iqbal, I., and Iqbal, K. (1995) Phosphatase activity toward abnormally phosphorylated Tau. Decrease in Alzheimer disease brain. *J. Neurochem.* **65,** 732–738
24. Wang, J. Z., Grundke-Iqbal, I., and Iqbal, K. (2007) Kinases and phosphatases and Tau sites involved in Alzheimer neurofibrillary degeneration. *Eur. J. Neurosci.* **25,** 59–68
25. Adachi, Y., Pavlakis, G. N., and Copeland, T. D. (1994) Identification and characterization of SET, a nuclear phosphoprotein encoded by the translocation break point in acute undifferentiated leukemia. *J. Biol. Chem.* **269,** 2258–2262
26. ten Klooster, J. P., Leeuwen, I., Scheres, N., Anthony, E. C., and Hordijk, P. L. (2007) Rac1-induced cell migration requires membrane recruitment of the nuclear oncogene SET. *EMBO J.* **26,** 336–345
27. Lam, B. D., Anthony, E. C., and Hordijk, P. L. (2012) Analysis of nucleocytoplasmic shuttling of the proto-oncogene SET/I2PP2A. *Cytometry A* **81,** 81–89
28. Canela, N., Rodriguez-Vilarrupla, A., Estanyol, J. M., Diaz, C., Pujol, M. J., Agell, N., and Bachs, O. (2003) The SET protein regulates G_2/M transition by modulating cyclin B-cyclin-dependent kinase 1 activity. *J. Biol. Chem.* **278,** 1158–1164
29. Compagnone, N. A., Zhang, P., Vigne, J. L., and Mellon, S. H. (2000) Novel role for the nuclear phosphoprotein SET in transcriptional activation of P450c17 and initiation of neurosteroidogenesis. *Mol. Endocrinol.* **14,** 875–888
30. Seo, S. B., McNamara, P., Heo, S., Turner, A., Lane, W. S., and Chakravarti, D. (2001) Regulation of histone acetylation and transcription by INHAT, a human cellular complex containing the set oncoprotein. *Cell* **104,** 119–130
31. Madeira, A., Pommet, J. M., Prochiantz, A., and Allinquant, B. (2005) SET protein (TAF1β, I_2^{PP2A}) is involved in neuronal apoptosis induced by an amyloid precursor protein cytoplasmic subdomain. *FASEB J.* **19,** 1905–1907
32. Tanimukai, H., Grundke-Iqbal, I., and Iqbal, K. (2005) Up-regulation of inhibitors of protein phosphatase-2A in Alzheimer's disease. *Am. J. Pathol.* **166,** 1761–1771
33. Arnaud, L., Chen, S., Liu, F., Li, B., Khatoon, S., Grundke-Iqbal, I., and Iqbal, K. (2011) Mechanism of inhibition of PP2A activity and abnormal

hyperphosphorylation of Tau by I_2^{PP2A}/SET. *FEBS Lett.* **585,** 2653–2659
34. Wang, X., Blanchard, J., Kohlbrenner, E., Clement, N., Linden, R. M., Radu, A., Grundke-Iqbal, I., and Iqbal, K. (2010) The carboxy-terminal fragment of inhibitor-2 of protein phosphatase-2A induces Alzheimer disease pathology and cognitive impairment. *FASEB J.* **24,** 4420–4432
35. Bolognin, S., Blanchard, J., Wang, X., Basurto-Islas, G., Tung, Y. C., Kohlbrenner, E., Grundke-Iqbal, I., and Iqbal, K. (2012) An experimental rat model of sporadic Alzheimer's disease and rescue of cognitive impairment with a neurotrophic peptide. *Acta Neuropathol.* **123,** 133–151
36. Graham, J. (2001) Subcellular fractionation and isolation of organelles. Isolation of lysosomes from tissues and cells by differential and density gradient centrifugation. *Curr. Protoc. Cell Biol.* **3.6,** 1–21
37. Gong, C. X., Lidsky, T., Wegiel, J., Grundke-Iqbal, I., and Iqbal, K. (2001) Metabolically active rat brain slices as a model to study the regulation of protein phosphorylation in mammalian brain. *Brain Res. Brain Res. Protoc.* **6,** 134–140
38. Chohan, M. O., Khatoon, S., Iqbal, I. G., and Iqbal, K. (2006) Involvement of I_2^{PP2A} in the abnormal hyperphosphorylation of Tau and its reversal by Memantine. *FEBS Lett.* **580,** 3973–3979
39. Grundke-Iqbal, I., Iqbal, K., Tung, Y. C., Quinlan, M., Wisniewski, H. M., and Binder, L. I. (1986) Abnormal phosphorylation of the microtubule-associated protein Tau (τ) in Alzheimer cytoskeletal pathology. *Proc. Natl. Acad. Sci. U.S.A.* **83,** 4913–4917
40. Seubert, P., Mawal-Dewan, M., Barbour, R., Jakes, R., Goedert, M., Johnson, G. V., Litersky, J. M., Schenk, D., Lieberburg, I., and Trojanowski, J. Q. (1995) Detection of phosphorylated Ser in fetal Tau, adult Tau, and paired helical filament Tau. *J. Biol. Chem.* **270,** 18917–18922
41. Morgan, J. M., Navabi, H., Schmid, K. W., and Jasani, B. (1994) Possible role of tissue-bound calcium ions in citrate-mediated high-temperature antigen retrieval. *J. Pathol.* **174,** 301–307
42. Tsujio, I., Zaidi, T., Xu, J., Kotula, L., Grundke-Iqbal, I., and Iqbal, K. (2005) Inhibitors of protein phosphatase-2A from human brain structures, immunocytological localization and activities towards dephosphorylation of the Alzheimer type hyperphosphorylated Tau. *FEBS Lett.* **579,** 363–372
43. Iqbal, K., Flory, M., Khatoon, S., Soininen, H., Pirttila, T., Lehtovirta, M., Alafuzoff, I., Blennow, K., Andreasen, N., Vanmechelen, E., and Grundke-Iqbal, I. (2005) Subgroups of Alzheimer's disease based on cerebrospinal fluid molecular markers. *Ann. Neurol.* **58,** 748–757
44. Kreuzaler, P. A., Staniszewska, A. D., Li, W., Omidvar, N., Kedjouar, B., Turkson, J., Poli, V., Flavell, R. A., Clarkson, R. W., and Watson, C. J. (2011) Stat3 controls lysosomal-mediated cell death in vivo. *Nat. Cell Biol.* **13,** 303–309
45. Alonso, A., Zaidi, T., Novak, M., Grundke-Iqbal, I., and Iqbal, K. (2001) Hyperphosphorylation induces self-assembly of Tau into tangles of paired helical filaments/straight filaments. *Proc. Natl. Acad. Sci. U.S.A.* **98,** 6923–6928
46. Glunde, K., Guggino, S. E., Solaiyappan, M., Pathak, A. P., Ichikawa, Y., and Bhujwalla, Z. M. (2003) Extracellular acidification alters lysosomal trafficking in human breast cancer cells. *Neoplasia* **5,** 533–545
47. Back, T., Hoehn, M., Mies, G., Busch, E., Schmitz, B., Kohno, K., and Hossmann, K. A. (2000) Penumbral tissue alkalosis in focal cerebral ischemia. Relationship to energy metabolism, blood flow, and steady potential. *Ann. Neurol.* **47,** 485–492
48. Chen, J. M., Fortunato, M., and Barrett, A. J. (2000) Activation of human prolegumain by cleavage at a C-terminal asparagine residue. *Biochem. J.* **352,** 327–334
49. Nixon, R. A., Cataldo, A. M., and Mathews, P. M. (2000) The endosomal-lysosomal system of neurons in Alzheimer's disease pathogenesis. A review. *Neurochem. Res.* **25,** 1161–1172
50. Yang, A. J., Chandswangbhuvana, D., Margol, L., and Glabe, C. G. (1998) Loss of endosomal/lysosomal membrane impermeability is an early event in amyloid Aβ1–42 pathogenesis. *J. Neurosci. Res.* **52,** 691–698
51. Castellani, R. J., Honda, K., Zhu, X., Cash, A. D., Nunomura, A., Perry, G., and Smith, M. A. (2004) Contribution of redox-active iron and copper to oxidative damage in Alzheimer disease. *Ageing Res. Rev.* **3,** 319–326
52. Li, M., Guo, H., and Damuni, Z. (1995) Purification and characterization of two potent heat-stable protein inhibitors of protein phosphatase 2A from bovine kidney. *Biochemistry* **34,** 1988–1996
53. Katayose, Y., Li, M., Al-Murrani, S. W., Shenolikar, S., and Damuni, Z. (2000) Protein phosphatase 2A inhibitors, I_1^{PP2A} and I_2^{PP2A}, associate with and modify the substrate specificity of protein phosphatase 1. *J. Biol. Chem.* **275,** 9209–9214
54. Turk, B., Dolenc, I., Turk, V., and Bieth, J. G. (1993) Kinetics of the pH-induced inactivation of human cathepsin L. *Biochemistry* **32,** 375–380
55. Pivtoraiko, V. N., Stone, S. L., Roth, K. A., and Shacka, J. J. (2009) Oxidative stress and autophagy in the regulation of lysosome-dependent neuron death. *Antioxid. Redox Signal.* **11,** 481–496
56. Pratt, M. R., Sekedat, M. D., Chiang, K. P., and Muir, T. W. (2009) Direct measurement of cathepsin B activity in the cytosol of apoptotic cells by an activity-based probe. *Chem. Biol.* **16,** 1001–1012
57. Miura, Y., Sakurai, Y., Hayakawa, M., Shimada, Y., Zempel, H., Sato, Y., Hisanaga, S., and Endo, T. (2010) Translocation of lysosomal cathepsin D caused by oxidative stress or proteasome inhibition in primary cultured neurons and astrocytes. *Biol. Pharm. Bull.* **33,** 22–28